≪Research Paper≫ Applied Science and Convergence Technology Vol.24 No.4, July 2015, pp.117~124
http://dx.doi.org/10.5757/ASCT.2015.24.4.117

Direct Growth of Graphene on Insulating Substrate by Laminated (Au/Ni) Catalyst Layer

Yong Hun Ko[a], Yooseok Kim[b], Daesung Jung[c], Seung Ho Park[a], Ji Sun Kim[a], Jini Shim[a], Hyeju Yun[a], Wooseok Song[d], and Chong-Yun Park[a]*

[a]*Department of Physics, Sungkyunkwan University, Suwon 16419, Korea*
[b]*Advanced Nano-Surface Research Group, Korea Basic Science Institute (KBSI), Daejeon 305-333, Korea*
[c]*Department of Energy Science, Sungkyunkwan University, Suwon 16419, Korea*
[d]*Thin Film Materials Laboratory, Korea Research Institute of Chemical Technology, Daejeon 305-600, Korea*

(Received July 28, 2015, Revised July 29, 2015, Accepted July 29, 2015)

A direct growth method of graphene on insulating substrate without catalyst etching and transfer process was developed using Au/Ni/a-C catalyst system. During the growth process, behavior of the Au/Ni catalyst was investigated using EDX, XPS, SEM, and Raman spectroscopy. The Au/Ni catalyst layer was evaporated during growth process of graphene. The graphene film was composed mono-layer flakes. The transmittance of the graphene film was ~80.6%.

Keywords : Graphene, Direct growth, Eutectic temperature, Amorphous carbon

I. Introduction

Graphene, a two-dimensional material composed of sp^2 carbon atoms with compact honeycomb lattice, has attracted much attention due to its excellent physical properties such as extremely high carrier mobility (200,000 cm^2/Vs) and ballistic transport properties [1,2]. For the past few years, chemical vapor deposition (CVD) method has been widely used for growth of large-area uniform graphene on catalytic metals such as Cu or Ni foils [3-8]. However, the graphene synthesized on metals by the CVD method must be transferred to insulating substrates for device applications [9-15]. Although considerable progress has been made in transfer process, wrinkles and cracks, degrading the electrical and optical properties, are still caused in the graphene [16-19]. Thus, a direct growth method of graphene on insulating substrates has been studied.

Recently, the several methods were developed using mixed amorphous carbon (a-carbon) and catalytic metal thin film or catalytic metal/a-carbon thin film on insulating substrate [20-25]. However, those methods still require catalyst etching process after growth of graphene. Therefore, it has become a very important task to develop a method for removing catalytic film during growth process of graphene, simultaneously.

In this work, we report a new approach for direct growth graphene using evaporation of Au-Ni alloy at low temperature due to lower eutectic temperature [26]. First of all, an Au/Ni/quartz samples were

* [E-mail] cypark@skku.edu

prepared by magnetron sputtering and annealed at processing temperature. The mono- and bi-layer graphene were synthesized on quartz plate without catalyst etching process and evaluated by Raman spectroscopy, optical microscopy, scanning electron microscopy (SEM), optical transmittance spectrophotometer (OTS), X-ray photoelectron spectroscopy (XPS).

II. Experimental Section

1. Growth of graphene

The 1×1 cm^2 quartz plate was first cleaned using ultra-sonication in ethanol and acetone for 5 min, respectively. An a-C (0.5 nm thick, 99.99%) layer was deposited on a clean quartz plate. Subsequently, Ni (60 nm thick, 99.99%) and Au (10～30 nm thick, 99.99%) layers were also deposited by direct-current (DC) magnetron sputtering. The Au/Ni/a-C/quartz plates were then loaded into a CVD chamber and heated up to 1100°C for 3 min in an H_2 atmosphere (Fig. 1). After cooling the chamber to room temperature, the quartz plate was taken out for characterization without further post treatments.

2. Graphene characterization

The graphene film was characterized by a Raman spectroscope (Renishaw, RM1000 inVia) with an excitation wavelength of 532 nm and a laser spot size of 5 μm. The surface morphology of graphene was observed by an optical microscopy and a field-emission scanning electron microscopy (FE-SEM, JSM7000F of JEOL corporation). The surface component of graphene was investigated by X-ray photoelectron spectroscopy (XPS, VGMICROTECH, ESCA 2000, monochromatic Al Kα radiation (hν=1486.6 eV)) and an energy-dispersive X-ray spectroscopy (EDX, JEOL, JSM 7000F, accelerating voltage of 1 kV).

III. Results and Discussion

Graphene has been synthesized using Ni/amorphous-Carbon-coated transparent quartz (Ni/a-C/

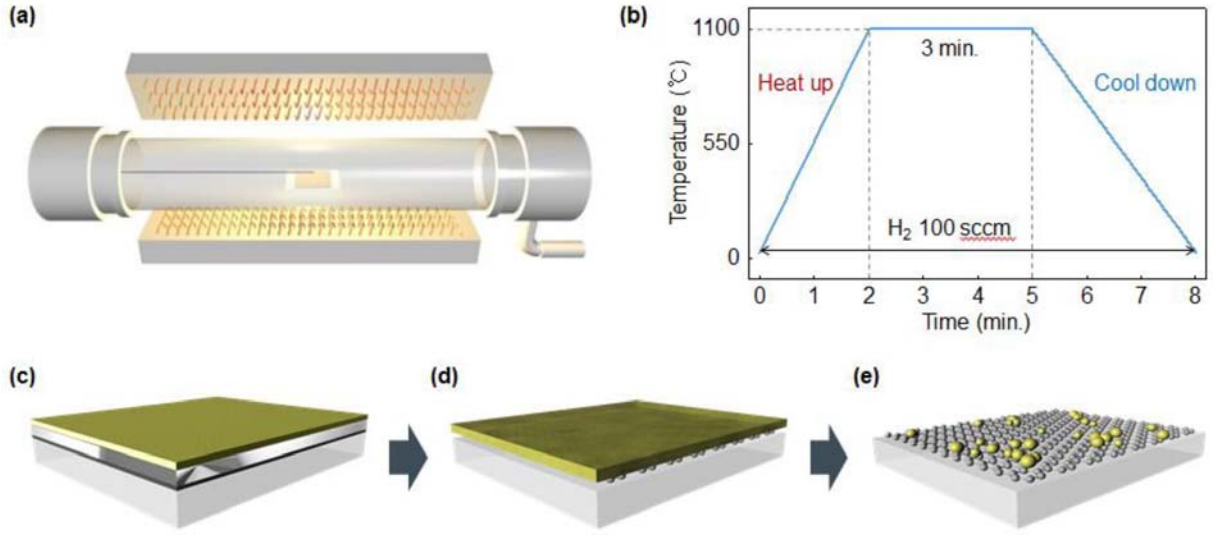

Figure 1. (a) Schematic image of thermal annealing system. (b) Growth process of graphene using thermal annealing system. (c)～(e) Schematic growth process of graphene on quartz. (c) as prepared a catalyst system on quartz, (d) during growth, (e) after growth.

quartz) substrate to investigate the growth conditions such as growth and time temperature, and thickness of Ni and a-C film (Supporting Information, Fig. S1). Fig. 2(a) shows the SEM image of the graphene synthesized on quartz plate under the optimized growth condition. Fig. 2(b) and 2(c) shows two typical Raman and EDX spectra, respectively, taken from blue and green dashed circles in Fig. 2(a). The typical graphene peaks at 1582 (G band), 2701 (2D band) cm^{-1}, and weak D band at 1358 cm^{-1} from the both bright and dark regions in Fig. 2(a) show that large-area graphene was synthesized on quartz [26,27]. The bright region (green dashed region in Fig. 2(c)) on the SEM image was identified as nickel particles by EDX measurement. It reveals that nickel of 9.09% in atomic percent remained. (Supporting Information, Table S1). Transmittance of the graphene film was 26.5% at 550 nm of wavelength as shown in Fig. 2(d). It is significantly low and would be due to the residual nickel particles. Although most of the nickel particles was removed by etching process to atomic percentage of 0.28% (Supporting Information, Table S1), other defects were generated during process.

To overcome this problem, new catalyst system to eliminate catalyst etching process was required. Thus, we searched a Ni-alloy with low eutectic temperature and evaporation point. As a result, Au (0~50%)-Ni alloy was adopted as catalytic layer. The melting point of Au (0~60%)-Ni alloy was lowered less than 1100°C (Supporting Information, Fig. S2) [25]. Fig. 3(a)~3(d) show optical images of the graphene films synthesized using the catalyst system Au (0~30 nm)/Ni/a-C/quartz plates, Scale bar: 30 μm. It was observed that transmittance of graphene

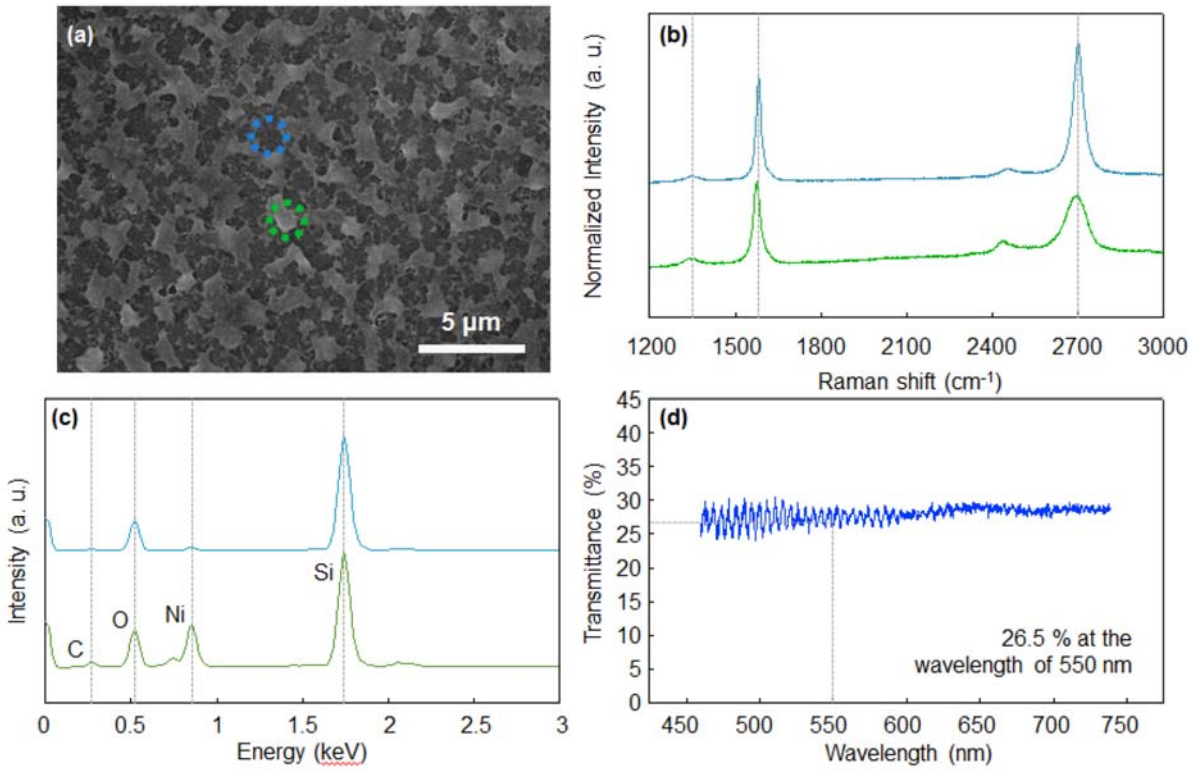

Figure 2. (a) SEM image of graphene on quartz synthesized by annealing Ni/a-C/quartz. (b) Typical Raman spectrum taken from blue and green dashed circles in Figure 1(a). (c) EDX spectrum of graphene before (green line) and after (blue line) nickel etching. (d) Optical transmittance spectrum of graphene, showing low transmittance due to remained nickel particles.

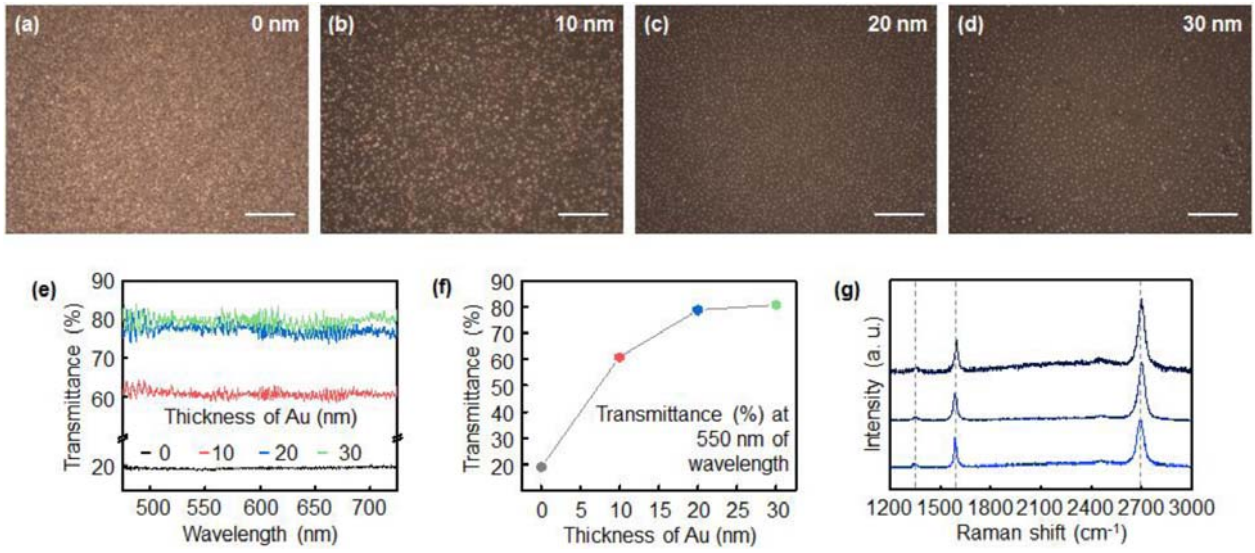

Figure 3. (a)~(d) Optical images and (e), (f) transmittance of the graphene films synthesized with Au layer of (a) 0, (b) 10, (c) 20, (d) 30 nm. (g) Raman spectrum of the graphene film synthesized with Au layer of 30 nm.

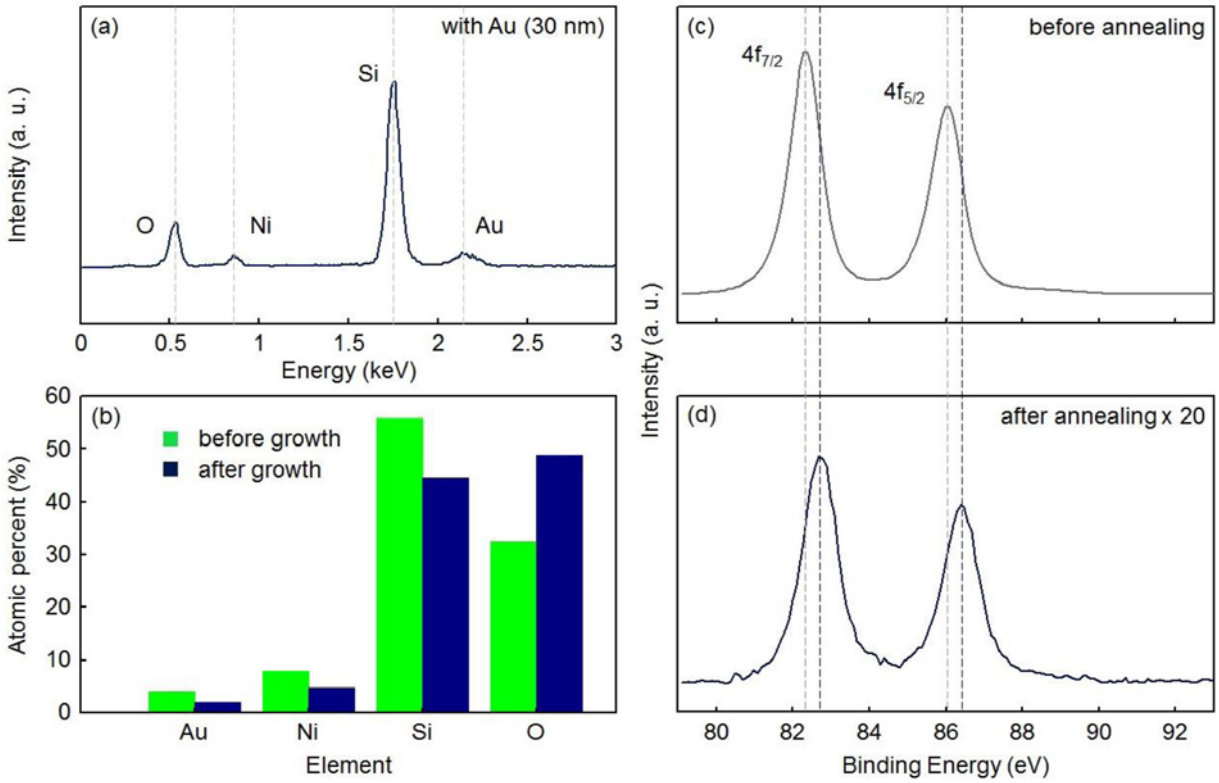

Figure 4. (a) EDX spectra of graphene showing low intensity of Ni and Au. (b) Atomic percent of each component before and after growth of graphene. (c) and (d) XPS data showing high-binding shift of Au 4f peaks and decreased peak intensity after growth of graphene.

was improved as the thickness of Au layer increased as shown in Fig. 3(e). Fig. 3(f) shows the evolution of optical transmittance at 550 nm of wavelength of the graphene films to several Au-thickness. The optical transmittance was maximized at 30 nm Au and ~80.6%, which means the residual amount of Au-Ni

alloy reached to minimum at 30 nm Au (Supporting Information, Table S2). Raman spectra in Fig. 3(g) show that monolayer graphene film was synthesized on quartz plate in most of areas [27,28].

To check the actual decrease of amount of Ni as well as Au, EDX and XPS measurement was conducted. Fig. 4(a) shows EDX spectrum of the graphene film synthesized by using the Au/Ni/a-C/quarts catalyst system with Au (30 nm) layer. Significant decrease of Ni peak intensity was observed as well as week Au peak intensity. XPS spectra of Au $4f_{7/2}$ and $4f_{5/2}$ core levels at 82.38 eV and 86.08 eV, respectively, (c) before and (d) after growth of graphene in Fig. 4(c) and 4(d), show drastic decrease in amount of Au in the graphene film. The high-binding shift (+0.3 eV) of Au peaks is attributed to formation of Au-Ni alloy [29]. To confirm that evaporation of Ni film was resulted by formation of Au-Ni alloy, we analyzed the change in EDX intensity of each component such as Au, Ni, Si, and O atoms. Fig. 4(b) shows the atomic percentage of Au, Ni, Si, and O. The atomic percent of Au was measured ~4% before growth of graphene. After growth of graphene film, Au and Ni atomic percent drastically decreased. It indicates that residual Ni amount after growth of graphene was reduced significantly as using the Au/Ni/a-C catalyst system, which is agree with the transmittance data.

IV. Conclusions

In this work, we have developed a new catalyst system for graphene growth on insulating substrate. The graphene film was synthesized directly the graphene film using the Au (30 nm)/Ni/a-C/ system on a quartz plate through typical growing process of graphene. The graphene film composed of mon-layer flakes on quartz plate was obtained without catalyst etching and graphene transfer process. Transmittance of the graphene film was 80.6% at the wavelength of 550 nm.

Acknowledgements

This work was supported by the Basic Science Research Program (2013-008639) through the National Research Foundation of Korea (NRF), funded by the Ministry of Education, Science and Technology. W. Song and K.-S. An were supported by a grant (2011-0031636) from the Center for Advanced Soft Electronics under the Global Frontier Research Program of the Ministry of Education, Science and Technology, Korea.

References

[1] K. S. Novoselov, A. K. Geim, S. V. Morozov, D. Jiang, Y. Zhang, S. V. Dubonos, I. V. Grigorieva, and A. A. Firsov, Science, **306**, 666 (2004).

[2] A. K. Geim, and K. S. Novoselov, Nature Mater., **6**, 183 (2007).

[3] A. Reina, X. Jia, J. Ho, D. Nezich, H. Son, V. Bulovic, M. S. Dresselhaus, and J. Kong, Nano Lett., **9**, 30 (2008).

[4] X. Li, W. Cai, J. An, S. Kim, J. Nah, D. Yang, R. Piner, A. Velamakanni, I. Jung, E. Tutuc, S. K. Banerjee, L. Colombo, R. S. Ruoff, Science, **324**, 1312 (2009).

[5] M. G. Rybin, A. S. Pozharov, and Elena D. Obraztsova, Phys. Status Solidi C, **7**, 2785 (2010).

[6] W. Song, C Jeon , S. Y. Kim, Y Kim, S. H Kim, Su-Il Lee, D. S. Jung, M. W. Jung, K. S. An, and C. -Y. Park, C arbon, **68**, 87 (2014).

[7] T. Kobayashi, M. Bando, N. Kimura, K. Shimizu, K. Kadono, N. Umezu, K. Miyahara, S. Hayazaki, S. Nagai, Y. Mizuguchi, Y. Murakami, and D. Hobara, Appl. Phys. Lett., **102**, 023112 (2011).

[8] K. Yan, H. Peng, Y. Zhou, H. Li, and Z. Liu, Nano Lett., **11**, 1106 (2011).

[9] Q. Sun, D. H. Kim, S. S. Park, N. Y. Lee, Y. Zhang, J. H. Lee, K. Cho, and J. H. Cho, Adv. Meter., **26**, 4735 (2014).

[10] E. Shi, H. Li, L. Yang, J. Hou, Y. Li, L. Li, A. Cao, and Y. Fang, Adv. Mater., **27**, 682 (2015).
[11] H. O. Choi, D. W. Kim, S. J. Kim, S. B .Yang, and H.-T. Jung, Adv. Mater., **26**, 4575 (2014).
[12] H. Lv, H. Wu, K. Xiao, W. Zhu, H. Xu, Z. Zhang, and H. Qian, Appl. Phys. Lett., **102**, 183107 (2013).
[13] Z. Liu, A. A. Bol, and W. Haensch, Nano Lett., **11**, 523 (2011).
[14] J. -Y. Kim, J. Lee, W. H. Lee, I. N. Kholmanov, J. W. Suk, T. Y. Kim, Y. Hao, H. Chou, D. Akinwande, and R. S. Ruoff, ACS Nano, **8**, 269 (2014).
[15] J. Park, W. H. Lee, S. Huh, S. H. Sim, S. B. Kim, K. Cho, B. H. Hong, and K. S. Kim, J. Phys. Chem. Lett., **2**, 841 (2011).
[16] X. Liang, B. A. Sperling, I. Calizo, G. Cheng, C. A. Hacker, Q. Zhang, Y. Obeng, K. Yan, H. Peng, Q. Li, X. Zhu, H. Yuan, A. R. H. Walker, Z. Liu, L. Peng, and C. A. Richter, **5**, 9144 (2011).
[17] M. Her, R. Beams, and L. Novotny, Phys. Lett. A, **377**, 1455 (2013).
[18] W. Jung, D. Kim, M. Lee, S. Kim, J. -H. Kim, and C. -S. Han, Adv. Mater., **26**, 6394 (2014).
[19] H. H. Kim, Y. Chung, E. Lee, S. K. Lee, and K. Cho, Adv. Mater, **26**, 3213 (2014).
[20] K. Banno, M. Mizuno, K. Fujita, T. Kubo, M. Miyoshi, T. Egawa, and T. Soga, **103**, 082112 (2013).
[21] T. Ikuta, K. Gumi, Y. Ohno, K. Maehashi, K. Inoue, and K. Matsumoto, Material Research Express, **1**, 025028 (2014).
[22] X. Liu, T. Lin, M. Zhou, H. Bi, H. Cui, D. Wan, F. Huang, and J. Lin, Carbon, **71**, 20 (2014).
[23] Z. Peng, Z. Yan, Z. Sun, and J. M. Tour, ACS Nano, **5**, 8241 (2011).
[24] Z. Yan, Z. Peng, Z. Sun, J. Yao, Y. Zhu, Z. Liu, P. M. Ajayan, and J. M. Tour, ACS Nano, **5**, 8187 (2011).
[25] A. Delamoreanu, C. Robot, C. Vallee, and A. Zenasni, Carbon, **66**, 48 (2014).
[26] Z. Yang, D. J. Lichtenwalner, A. S. Morris, J. Krim, and A. I. Kingon, IEEE Journals & Magazines, **18**, 287 (2009).
[27] M. S. Dresselhaus, A. Jorio, M. Hofmann, G. Dresselhaus, and R. Saito, Nano Lett., **10**, 751 (2010).
[28] L. M. Malard, M. A. Pimenta, G. Dresselhaus, M. S. Dresselhaus, Phys. Report, **473**, 51 (2009).
[29] L. Zhao, N. Heinig, and K. T. Leung, J. Phys. Chem. C, **116**, 12322 (2012).

Supporting Information

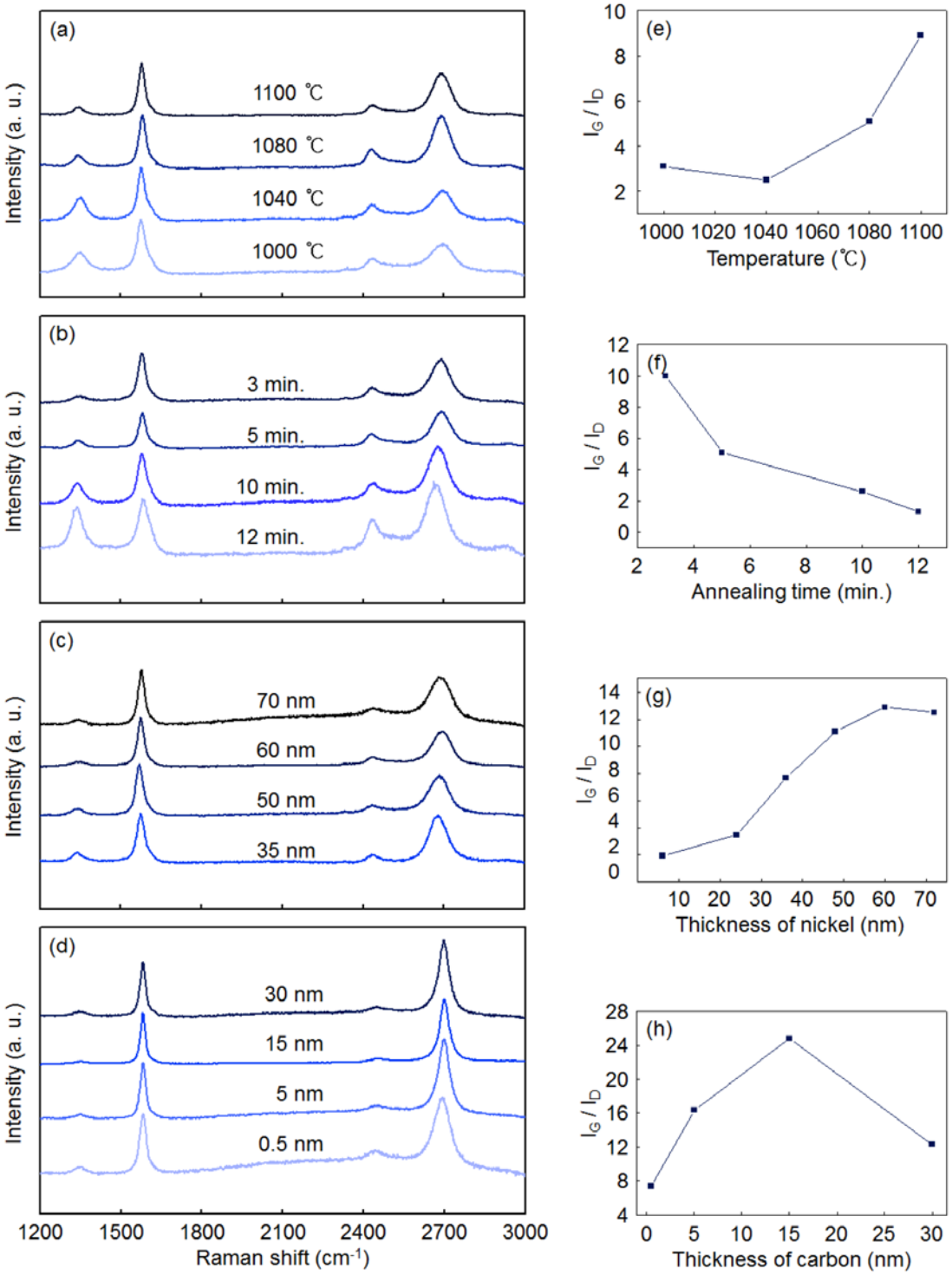

Figure S1. (a)~(d) Raman spectrum of graphene synthesized in varying (a) growth temperature and (b) time, thickness of (c) Ni and (d) a-C. (e)~(h) G-D peak intensity ratio of graphene versus (e) growth temperature and (f) time, thickness of (g) Ni and (h) a-C.

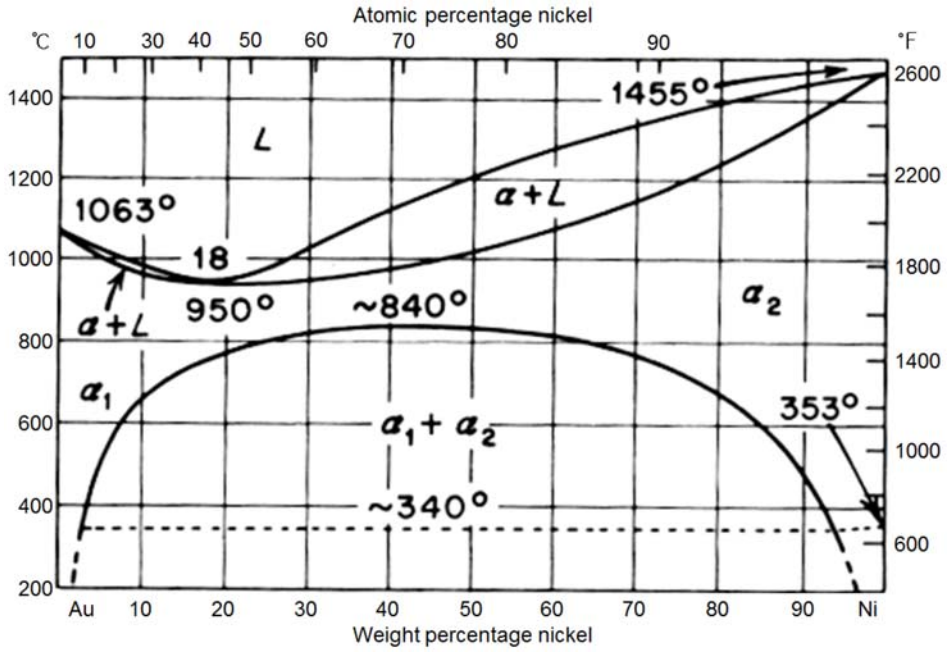

Figure S2. Gold–nickel phase diagram.

Table S1. Atomic percentage of each component before and after nickel etching.

Element	Atomic % (before etching)	Atomic % (after etching)
C	27.81	16.59
O	43.63	57.20
Si	19.47	25.93
Ni	9.09	0.28

Table S2. Transmittance of graphene on quartz in varying thickness of Au.

Thickness of Au (nm)	Transmittance (%)
0	19.01
10	60.83
20	78.73
30	80.60